

Electric Dipole Induced Spin Resonance in Quantum Dots

Vitaly N. Golovach, Massoud Borhani, and Daniel Loss

Department of Physics and Astronomy, University of Basel, Klingelbergstrasse 82, 4056 Basel, Switzerland

(Dated: September 26, 2018)

An alternating electric field, applied to a quantum dot, couples to the electron spin via the spin-orbit interaction. We analyze different types of spin-orbit coupling known in the literature and find two efficient mechanisms of spin control in quantum dots. The linear in momentum Dresselhaus and Rashba spin-orbit couplings give rise to a fully transverse effective magnetic field in the presence of a Zeeman splitting at lowest order in the spin-orbit interaction. The cubic in momentum Dresselhaus terms are efficient in a quantum dot with non-harmonic confining potential and give rise to a spin-electric coupling proportional to the orbital magnetic field. We derive an effective spin Hamiltonian, which can be used to implement spin manipulation on a timescale of 10 ns with the current experimental setups.

PACS numbers: 73.23.Hk, 73.63.Kv

I. INTRODUCTION

Coherent manipulation of electron spin is at the heart of spintronics^{1,2} and quantum computing with spins.³ In the proposal of Ref. 3, the spin of an electron confined to a quantum dot is used as qubit to store and process quantum information. A quantum register consisting of an array of such spin-1/2 quantum dots is operated by a set of quantum gates that act on single spins and pairs of neighboring spins.³ Among the simplest quantum gates are the spin rotations on the Bloch sphere. With the help of only a static magnetic field and an electron-spin-resonance (ESR) pulse, one can change the state of the spin qubit at will. It is important, however, that the ESR pulse can be applied locally to each of the quantum dots, ensuring that the spins are accessed independently from one another. For an ESR^{4,5} to occur, usually, the electron is exposed to an alternating magnetic field of a frequency ω_{ac} that matches the electron Zeeman splitting. However, because strong local electric fields are easier to obtain than strong local magnetic fields, interest arises in spin resonance induced by electric fields.

Recently, Kato *et al.*⁶ have demonstrated three-dimensional control of spins in a GaAs/Al_xGa_{1-x}As heterostructure with the use of an alternating electric field. The mechanism of spin coupling to the electric field relies on a specially engineered Landé g tensor in the heterostructure, achieved by modulating the Al content during the MBE growth.⁷ The resulting g tensor is both anisotropic and space-dependent, and allows control over the direction and magnitude of the spin precession frequency.^{6,8} A g -factor modulation resonance (g -TMR) occurs similarly to an ESR, when the frequency of the electric field matches the Zeeman splitting.⁶ Rashba and Efros⁹ have further proposed to use the standard (Dresselhaus¹⁰ and Rashba¹¹) spin-orbit couplings to achieve an electric dipole induced spin resonance (EDSR) in quantum wells. Rashba and Efros⁹ have shown that the EDSR is highly efficient in quantum wells, promising electron spin control on a timescale $\omega_R^{-1} \simeq 100$ ps, where ω_R is the Rabi frequency.⁴ These results have im-

portant practical implications in spintronics, where spins of extended electrons are used as a resource to accomplish information processing. In the context of quantum computing, however, interest arises in the spin of a localized electron. A natural question is, therefore, “What is the microscopic mechanism of EDSR in quantum dots and how strong is the EDSR effect?”

EDSR has nearly half-a-century long history. It has been first observed for extended electrons in bulk semiconductors,^{12,13} and studied more recently for donor-bound electrons in Cd_{1-x}Mn_xSe¹⁴ and extended electrons in two-dimensional electron gases^{15,16} and epilayers.¹⁷ The “forbidden” electric-dipole transition between the electron spin-up and spin-down states becomes possible in the presence of spin-orbit interaction. Absorption spectra of EDSR provide information about the value of the electron g factor and the strength of the spin-orbit coupling. In two-dimensional electron systems, one expects the Dresselhaus spin-orbit interaction¹⁰ to be enhanced compared to bulk semiconductors, because of the confinement of electron motion in one direction. Furthermore, the Rashba spin-orbit interaction¹¹ arises in heterostructures lacking inversion symmetry, such as, e.g., heterojunctions. In some systems, the Rashba coupling constant can be efficiently tuned by electric fields.¹⁸

In quantum dots,¹⁹ the spin-orbit interaction is generally suppressed due to complete localization of electron motion.²⁰ Typically, the quantum dot lateral size λ_d is smaller than the spin-orbit length λ_{SO} , and any effect of the spin-orbit interaction is suppressed as a power of λ_d/λ_{SO} and therefore is expected to be weak. This expectation contrasts with the case of electrons in quantum wells, where the EDSR meets most favorable conditions.⁹ The Zeeman interaction in quantum dots plays an important role for observing spin-orbit effects.^{21,22} Without the Zeeman interaction, the Rashba and linear in momentum Dresselhaus spin-orbit terms do not contribute to spin-related phenomena at the first order of spin-orbit interaction. This “absence of spin-orbit” at the leading order in quantum dots has been discussed extensively in the literature.^{20,21,22} Below, we show that a similar result arises

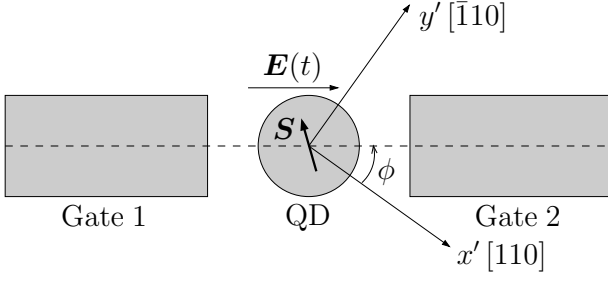


FIG. 1: Schematic of a setup for electric field control of spin via the spin-orbit interaction. The quantum dot (QD) contains a single electron with spin $\mathbf{S} = (\hbar/2)\boldsymbol{\sigma}$, deep in the Coulomb blockade valley. The gates 1 and 2 are used to generate an alternating electric field $\mathbf{E}(t)$, which acts via the spin-orbit interaction on the electron spin. As a result, an electric dipole spin resonance (EDSR) occurs if the frequency of $\mathbf{E}(t)$ is tuned to match the Larmor frequency $\omega_Z = E_Z/\hbar$.

also for the cubic in momentum Dresselhaus terms in the case when the dot confining potential is quadratic and the perturbation is linear in the electron coordinates.

In this paper, we consider the use of EDSR for control of individual electron spins in quantum dots. We derive an effective spin Hamiltonian for a quantum-dot electron, subject to *ac* electric fields. We show that there are two major mechanisms of EDSR in quantum dots. One arises from the linear in momentum Dresselhaus and Rashba spin-orbit couplings in combination with the Zeeman interaction. The other arises from the cubic Dresselhaus terms in combination with the cyclotron frequency. We estimate the strengths of both EDSR effects and compare them to the ordinary ESR. We find that despite a strong suppression, compared to quantum wells, the EDSR in quantum dots is still an efficient mechanism of spin manipulation and can be used alone or together with ESR to achieve control of spin on a timescale $\omega_R^{-1} \simeq 10$ ns.

II. EDSR SETUP

We consider a quantum dot containing a single electron with charge $-e$ and spin $\mathbf{S} = (\hbar/2)\boldsymbol{\sigma}$, where $\boldsymbol{\sigma} = (\sigma_x, \sigma_y, \sigma_z)$ are the Pauli matrices. The quantum dot is in the Coulomb blockade regime with extraction (U_-) and addition (U_+) energies that are large compared to the temperature, so that the dot occupation remains constant. An external electric field $\mathbf{E}(\mathbf{r}, t)$ is applied to the quantum dot. In practice, $\mathbf{E}(\mathbf{r}, t)$ can be generated by a pair of gates, as sketched in Fig. 1, to which an *ac* signal of frequency ω_{ac} is supplied from an external circuit (not shown). The Hamiltonian describing the quantum dot electron in the external alternating field reads

$$H = H_0 + V(\mathbf{r}, t), \quad (1)$$

where $V(\mathbf{r}, t) = e \int^{\mathbf{r}} d\mathbf{r}' \cdot \mathbf{E}(\mathbf{r}', t)$ is the potential energy of the electron in the external electric field and H_0 is the

“unperturbed” Hamiltonian (see further). In particular, for an electric field constant in space $\mathbf{E}(\mathbf{r}, t) = \mathbf{E}(t)$, the potential energy reads $V(\mathbf{r}, t) = e\mathbf{E}(t) \cdot \mathbf{r}$.

For practical applications, it is a good idea to use two gates, as shown in Fig. 1, because this allows larger amplitudes of $\mathbf{E}(t)$ to be applied to the quantum dot, while still maintaining the dot within the same Coulomb blockade valley. Ideally, the *ac* voltage drop is distributed between the two gates symmetrically and the dot potential is kept constant by counteracting potential shifts quadratic in the electric field. For a harmonic quantum dot, the desired *ac* potential reads

$$V(\mathbf{r}, t) = e\mathbf{E}(t) \cdot \mathbf{r} + \frac{(e\mathbf{E}(t))^2}{2m_e\omega_0^2}, \quad (2)$$

where m_e is the electron effective mass and ω_0 is the oscillator frequency. Then the only effect of the *ac* signal on the dot confinement is shifting the dot center as a function of time by the amount

$$\mathbf{r}_0(t) = -\frac{e\mathbf{E}(t)}{m_e\omega_0^2}. \quad (3)$$

The amplitude of $\mathbf{r}_0(t)$ is going to be a relevant parameter in our following analysis. Therefore, setups in which the dot can be easily moved on the substrate by gates are particularly interesting in the context of this paper. We discuss the case of $r_0 \sim \lambda_{SO}$ in Sec. VI, whereas for the bulk of the paper we restrict ourselves to $r_0 \ll \lambda_{SO}$.

The Hamiltonian H_0 consists of several terms,

$$H_0 = H_d + H_Z + H_{SO}, \quad (4)$$

where H_d is the Hamiltonian of a confined electron,

$$H_d = \frac{\mathbf{p}^2}{2m_e} + U(\mathbf{r}), \quad (5)$$

with $\mathbf{p} = -i\hbar\partial/\partial\mathbf{r} + (e/c)\mathbf{A}(\mathbf{r})$ being the electron momentum, c the speed of light in vacuum, and $U(\mathbf{r})$ the quantum dot confining potential. We restrict our consideration to quantum dots with strong confinement along one axis, such as, e.g., quantum dots defined in a two-dimensional electron gas (2DEG). For GaAs, the 2DEG lies, typically, in the crystallographic plane (001) and has a width $d \simeq 5$ nm, which ensures a strong size quantization along $z \parallel [001]$. The in-plane motion of the electron is described by the Hamiltonian (5), where $\mathbf{r} = (x, y)$ is the electron in-plane coordinate; whereas the transverse motion (along z) has already been integrated out in Eqs. (1)-(5). In the absence of external time-dependent fields, $\mathbf{A}(\mathbf{r})$ accounts for the orbital effect of a static magnetic field \mathbf{B} . Assuming that \mathbf{B} is constant in space, we have $\mathbf{A}(\mathbf{r}) = B_z(-y/2, x/2, 0)$ in the symmetric gauge. Note that the in-plane components B_x and B_y are not present in $\mathbf{A}(\mathbf{r})$, because the motion along z is strongly quantized ($d \ll \sqrt{\hbar c/eB_{x(y)}}$).

The magnetic field \mathbf{B} also induces a Zeeman splitting $E_Z = g\mu_B B$ and a spin quantization axis $\mathbf{n} = \mathbf{B}/B$ via

the Zeeman interaction,

$$H_Z = \frac{1}{2}g\mu_B \mathbf{B} \cdot \boldsymbol{\sigma} = \frac{1}{2}E_Z \mathbf{n} \cdot \boldsymbol{\sigma}, \quad (6)$$

where g is the electron g -factor and μ_B is the Bohr magneton. In GaAs, the magnitude of the g -factor is anomalously small ($g \approx -0.44$) compared to other A_{III}B_V semiconductors. The Zeeman energy is, therefore, much smaller than the cyclotron energy $\hbar\omega_c = \hbar eB_z/m_e c$ by a factor $gm_e/m \ll 1$ (with m being the electron mass in vacuum), for magnetic fields applied transversely to the 2DEG. In Sec. V, we derive an efficient spin-electric coupling that is proportional to $\hbar\omega_c$, but present only in non-harmonic quantum dots. We remark that the magnetic field is an important ingredient in our EDSR scheme, since at $B = 0$ no spin-electric coupling can be obtained at the first order of the spin-orbit interaction (see further).

In Eq. (4), H_{SO} stands for the spin-orbit Hamiltonian. We start with considering the so-called “linear in p ” spin-orbit interaction,

$$H_{SO} = \alpha(p_x\sigma_y - p_y\sigma_x) + \beta(-p_x\sigma_x + p_y\sigma_y), \quad (7)$$

which is the sum of the Rashba (α)¹¹ and 2D Dresselhaus (β)^{10,23} spin-orbit interactions. This type of spin-orbit interaction gives rise to a sizable phonon-induced spin relaxation rate $1/T_1$,^{21,22} of the same order of magnitude as experimentally measured.^{24,25,31} Moreover, in the 2D limit the linear in p spin-orbit interaction is dominant, because $\beta \propto 1/d^2$.

In the standard EDR scheme, an alternating magnetic field is generated by a current in a nearby conductor. In our setup (see Fig. 1), no charge flow is ideally present between the gates. However, the alternating electric field $\mathbf{E}(\mathbf{r}, z, t)$ gives rise to a displacement current, with the current density

$$\mathbf{J}_D(\mathbf{r}, z, t) = \frac{\kappa}{4\pi} \frac{\partial \mathbf{E}(\mathbf{r}, z, t)}{\partial t}, \quad (8)$$

where κ is the electric permittivity. The external magnetic field \mathbf{B} acquires, thus, an ac -component, $\mathbf{B} \rightarrow \mathbf{B} + \mathbf{B}(t)$, where $\mathbf{B}(t) = \nabla \times \mathbf{A}(t)$. The vector potential $\mathbf{A}(\mathbf{r}, z, t)$ is obtained as usual from Ampere’s law²⁶

$$\nabla^2 \mathbf{A} = -\frac{4\pi\mu}{c} (\mathbf{J} + \mathbf{J}_D), \quad (9)$$

where μ is the magnetic permittivity and \mathbf{J} is the charge flow density (in our case $\mathbf{J} = 0$). In Eq. (9), we adopted the Coulomb gauge $\nabla \cdot \mathbf{A} = 0$ and used the notation $\nabla = (\partial/\partial \mathbf{r}, \partial/\partial z)$.

The magnetic field $\mathbf{B}(t)$ couples to the electron spin via the Zeeman interaction in Eq. (6) [with $\mathbf{B} \rightarrow \mathbf{B} + \mathbf{B}(t)$], giving rise to an ESR source, which can be used, in principle, for spin manipulation in quantum dots. However, the amplitude of $\mathbf{B}(t)$ is, in practice, extremely small; it is proportional to $1/c$, as expected from the

relativistic nature of $\mathbf{B}(t)$. Furthermore, the proximity of the top gates to the 2DEG decrease the displacement current enclosed by the magnetic field lines penetrating the quantum dot. Using Eq. (9), we estimate $\mathbf{B} = \mu\kappa c^{-1} L_z \partial \mathbf{E}/\partial t \approx 10^{-6}$ G, for a quantum dot which is $L_z = 100$ nm below the gates plane and an electric field $E(t) = E_0 \sin(\omega_{ac}t)$, with amplitude $\mu\kappa E_0 = 10^2$ V/cm and frequency $\omega_{ac}/2\pi = 10^9$ Hz. As we show below, a much stronger effective magnetic field arises from the EDSR effect in the present setup, and therefore, the displacement current can be safely ignored.

Recently, a sizable ESR effect has been obtained with the help of a wire placed on top of a GaAs double dot.²⁷ In this case, $J \neq 0$ and the magnitude of $\mathbf{B}(t)$ is estimated from Eq. (9) to be $\mathbf{B} = \pi\mu c^{-1} I/(L_y + L_z)$, where I is current in the wire and $2L_y$ is the lateral size of the wire. For $L_y = L_z = 100$ nm and $I = 1$ mA, the magnetic field obtained in this setup is on the order of $\mathbf{B} \sim 10$ G.

III. SPIN-ELECTRIC COUPLING

Now, we focus on the electric-field component of the ac -signal and show that, together with the spin-orbit interaction H_{SO} and Zeeman splitting H_Z , it suffices to generate a sizable EDSR field in the quantum dot. For simplicity, we set $\mathbf{B}(t) \rightarrow 0$ from now on and choose $\mathbf{A}(t) = 0$. As a result, we retain only a constant in space and time magnetic field $\mathbf{B} = B(\cos\varphi \sin\vartheta, \sin\varphi \sin\vartheta, \cos\vartheta)$ and an alternating electric field $\mathbf{E}(\mathbf{r}, t) = (1/e)\nabla V(\mathbf{r}, t)$. Thus, we consider further the Hamiltonian in Eq. (1), assuming that H_0 is time-independent and describes the dot in the absence of ac fields.

We aim at diagonalizing H_0 using a Schrieffer-Wolff transformation, similar to Ref. 21. We thus look for a transformation matrix S such that the transformed Hamiltonian $\tilde{H}_0 = \exp(S)H_0 \exp(-S)$ is fully diagonal, see Appendix A. At $B = 0$, the ground state of H_0 (and also of \tilde{H}_0) is a Kramers doublet, because the spin-orbit interaction is always time-reversal symmetric (at $B = 0$). We therefore choose to encode the qubit into the ground state Kramers doublet of the quantum dot. Owing to the mixed spin and orbital nature of the states an alternating potential $V(\mathbf{r}, t)$, such as in Eq. (1), couples to the qubit. We proceed to derive this coupling, by calculating the transformation matrix S at the leading order of spin-orbit interaction,

$$S = \frac{1 - \mathcal{P}}{\hat{L}_d + \hat{L}_Z} H_{SO} + \mathcal{O}(H_{SO}^2), \quad (10)$$

where \hat{L}_d and \hat{L}_Z are Liouville superoperators, *i.e.* $\hat{L}_d A = [H_d, A]$ and $\hat{L}_Z A = [H_Z, A]$, $\forall A$. The projector \mathcal{P} projects onto the diagonal (or degenerate) part of the Hilbert space of $H_d + H_Z$, which ensures applicability of “non-degenerate” perturbation theory. The coupling of spin to electric fields is then found by applying

the same Schrieffer-Wolff transformation to the potential $V(\mathbf{r}, t)$. We obtain the following effective Hamiltonian for our qubit in the presence of an alternating potential $V(\mathbf{r}, t)$, to leading order in the spin-orbit interaction,

$$H_{\text{eff}} = H_Z + \langle \psi_0 | [S, V(\mathbf{r}, t)] | \psi_0 \rangle, \quad (11)$$

where S is the transformation matrix in Eq. (10) and $|\psi_0\rangle$ is the quantum dot ground state. For a quantum dot with a harmonic confining potential, $U(\mathbf{r}) = m_e \omega_0^2 r^2 / 2$, the transformation matrix S was calculated in Ref. 28 to all orders of the Zeeman interaction and the first order of the “linear in p ” spin-orbit interaction (7). For simplicity, we consider here only the linear in B terms,

$$\begin{aligned} S &= i\boldsymbol{\xi} \cdot \boldsymbol{\sigma} - \frac{E_Z}{m_e \omega_0^2} [\mathbf{n} \times \boldsymbol{\zeta}] \cdot \boldsymbol{\sigma}, \\ \boldsymbol{\xi} &= (\lambda_-^{-1} y', \lambda_+^{-1} x', 0), \\ \boldsymbol{\zeta} &= (\lambda_-^{-1} \partial/\partial y', \lambda_+^{-1} \partial/\partial x', 0), \end{aligned} \quad (12)$$

where $\lambda_{\pm} = \hbar/m_e(\beta \pm \alpha)$ are the spin-orbit lengths, and the vectors $\boldsymbol{\xi}$ and $\boldsymbol{\zeta}$ are given in the coordinate frame $x' = (x + y)/\sqrt{2}$, $y' = -(x - y)/\sqrt{2}$, and $z' = z$ (see Fig. 1). The first term in Eq. (12) commutes with scalar potentials and therefore drops out in Eq. (11). More generally, for arbitrary confining potential, the first term is replaced by $i(1 - \mathcal{P})\boldsymbol{\xi} \cdot \boldsymbol{\sigma}$, resulting nevertheless in no coupling of spin to electric fields. The second term in Eq. (12), however, allows us to express the coupling of spin to charge via the electric field $\mathbf{E}(t) = (1/e)\langle \psi_0 | \nabla V(\mathbf{r}, z, t) | \psi_0 \rangle$ that acts on the quantum dot electron. For the harmonic confining potential, we obtain

$$H_{\text{eff}} = \frac{1}{2} g \mu_B \mathbf{B} \cdot \boldsymbol{\sigma} + \frac{1}{2} \mathbf{h}(t) \cdot \boldsymbol{\sigma}, \quad (13)$$

$$\mathbf{h}(t) = 2g\mu_B \mathbf{B} \times \boldsymbol{\Omega}(t), \quad (14)$$

$$\boldsymbol{\Omega}(t) = \frac{-e}{m_e \omega_0^2} (\lambda_-^{-1} E_{y'}(t), \lambda_+^{-1} E_{x'}(t), 0). \quad (15)$$

The dimensionless field $\boldsymbol{\Omega}(t)$ describes a combined effect of the spin-orbit interaction and electric fields (or more generally potential fluctuations) on the qubit. $\boldsymbol{\Omega}(t)$ was calculated in Ref. 21 for the phonon potential and in Ref. 28 for the shot-noise of a QPC nearby the quantum dot. In our case, $\boldsymbol{\Omega}(t)$ is merely a classical driving field generated by the ac -signal.

Considering further a constant in space (at least on the scale of the quantum dot), alternating electric field $\mathbf{E}(t) = \mathbf{E}_0 \sin(\omega_{ac} t)$ of amplitude $\mathbf{E}_0 = E_0(\cos \phi, \sin \phi, 0)$, where ϕ is the angle of \mathbf{E}_0 with respect to the axis x' (see Fig. 1), we obtain explicitly $\boldsymbol{\Omega}(t) = \boldsymbol{\Omega}_0 \sin(\omega_{ac} t)$, with

$$\boldsymbol{\Omega}_0 = \frac{-e E_0}{m_e \omega_0^2} (\lambda_-^{-1} \sin \phi, \lambda_+^{-1} \cos \phi, 0). \quad (16)$$

To give an estimate for the amplitude Ω_0 in GaAs quantum dots, we assume $\lambda_+ \approx \lambda_- \approx \lambda_{SO} = 8 \mu\text{m}$, $\hbar\omega_0 = 1 \text{ meV}$, and $E_0 = 10^2 \text{ V/cm}$, which yields $\Omega_0 \sim 10^{-3}$.

The amplitude of the resulting effective magnetic field due to EDSR is found from Eq. (14) to be

$$\delta \mathbf{B}_0 = 2\mathbf{B} \times \boldsymbol{\Omega}_0. \quad (17)$$

The maximal amplitude is obtained for $\mathbf{B} \perp \boldsymbol{\Omega}_0$, which in experiment can easily be arranged for by, e.g., choosing $\mathbf{B} \parallel z$. In-plane magnetic fields can also be used, provided $\mathbf{E}(t)$ is linearly polarized. For example, an electric field $\mathbf{E}(t)$ aligned with x' generates, according to Eq. (15), a dimensionless field $\boldsymbol{\Omega}(t)$ along y' . In this case, \mathbf{B} should be chosen along x' for maximal spin-electric coupling.

Using our previous estimate for $\Omega_0 \sim 10^{-3}$, we obtain from Eq. (17) that $\delta B_0 \sim 1 \text{ mT}$ for a magnetic field $B = 1 \text{ T}$ oriented transversely to $\boldsymbol{\Omega}_0$. In principle, the dimensionless factor Ω_0 can be increased up to $\Omega_0 \sim 1$. However, this requires a specially designed setup, where the value of the electron displacement r_0 in Eq. (3) approaches the spin-orbit length λ_{SO} .

Next we remark that $\boldsymbol{\Omega}(t)$ in Eq. (15) can be written by the order of magnitude as $\Omega(t) \sim r_0(t)/\lambda_{SO}$. More rigorously, we rewrite Eq. (15) in the following form

$$\Omega_i(t) = \sum_j (\lambda_{SO}^{-1})_{ij} r_{0j}(t), \quad (18)$$

where $(\lambda_{SO}^{-1})_{ij}$ is a tensor of inverse spin-orbit lengths,

$$(\lambda_{SO}^{-1})_{ij} = \begin{pmatrix} 0 & 1/\lambda_- \\ 1/\lambda_+ & 0 \end{pmatrix}, \quad (19)$$

with $1/\lambda_{\pm} = m_e(\beta \pm \alpha)/\hbar$ and the frame (x', y') was used to represent the tensor. For order of magnitude estimates, it is useful to introduce the scalar

$$\frac{1}{\lambda_{SO}} = \frac{1}{\sqrt{2}} \|\lambda_{SO}^{-1}\|, \quad (20)$$

where $\|\lambda_{SO}^{-1}\|$ is the Frobenius norm of $(\lambda_{SO}^{-1})_{ij}$. In the case of Eq. (19), we have $1/\lambda_{SO} = (m_e/\hbar)\sqrt{\alpha^2 + \beta^2}$.

Despite the fact that Eq. (18) was obtained considering the harmonic confining potential as an example, its generality suggests that it should remain valid for quantum dots of arbitrary confinement, provided, to a good approximation, the ac -signal merely displaces the quantum dot parallel to itself by a vector $\mathbf{r}_0(t)$ as a function of time. Note that $\mathbf{r}_0(t)$ is the only available parameter to be compared with λ_{SO} in the limit of strong confinement ($\lambda_d \rightarrow 0$). We extend the class of Hamiltonians considered here to any combination of confinement and ac -voltage potential that can be rewritten in the form

$$U(\mathbf{r}) + V(\mathbf{r}, t) = U(\mathbf{r} - \mathbf{r}_0(t)) + V_0(t), \quad (21)$$

where $V_0(t)$ is independent of \mathbf{r} . We note that, as before, the electron wave function extension λ_d is assumed to be small compared to the spin-orbit length λ_{SO} at each moment in time. Equation (21) need not be satisfied exactly. Note that λ_d enters only in the definition of

$\mathbf{r}_0(t)$ and does appear alone as a parameter in Eq. (18). Therefore, defining $\mathbf{r}_0(t)$ as the average electron position, $\mathbf{r}_0(t) = \int \mathbf{r} |\psi(\mathbf{r}, t)|^2 d^2r$, we expect Eq. (18) to be valid to leading order also when the electron probability density $|\psi(\mathbf{r}, t)|^2$ changes shape, but the dot size changes weakly.

Equations (13), (14), and (18) form the basis of EDSR in quantum dots and can be used to efficiently manipulate the electron spin by electrical gates. Finally, we remark that Eqs. (13)-(15) have been derived under the assumption $r_0 \ll \lambda_{SO}$, and therefore, can be used only for $\Omega_0 \ll 1$. In Sec. VI we discuss the case of $\Omega_0 \sim 1$ in more detail. A further assumption in deriving Eqs. (13)-(15) was that the frequency spectrum of $\mathbf{E}(t)$ lies well below the size-quantization energy $\hbar\omega_0$. This adiabaticity constraint is generic to the spin-based quantum computation^{2,3}; it guarantees that the electron is not excited to higher in energy orbital levels.

IV. SPIN DYNAMICS AND COHERENCE

The electron spin obeys the Bloch equation^{29,30}

$$\langle \dot{\mathbf{S}} \rangle = [\boldsymbol{\omega}_Z + \delta\boldsymbol{\omega}(t)] \times \langle \mathbf{S} \rangle - \Gamma \langle \mathbf{S} \rangle + \boldsymbol{\Upsilon}, \quad (22)$$

where $\boldsymbol{\omega}_Z = g\mu_B \mathbf{B}/\hbar$ is the Larmor spin-precession frequency and $\delta\boldsymbol{\omega}(t) = \mathbf{h}(t)/\hbar$. The spin relaxation tensor Γ_{ij} and the inhomogeneous part Υ_i are due to the environment and can be derived microscopically^{21,29} within the Born-Markov approximation. Strictly speaking, Γ_{ij} and Υ_i in Eq. (22) depend also on the driving. In particular, Γ_{ij} acquires, in general, a time-dependent part. However, we neglect these effects here since the energy scales are well separated. Indeed, from experiments^{24,25,31} and theory,^{21,22} we infer that $\Gamma_{ij}, \Upsilon_i \sim (10^2 - 10^6) \text{ s}^{-1}$, *i.e.* they are very small, so that the regime $\Gamma_{ij}, \Upsilon_i \ll \delta\omega \ll \omega_Z$ holds. In this regime, the rotating wave approximation³⁰ is valid. We consider a completely general driving field

$$\delta\boldsymbol{\omega}(t) = \delta\boldsymbol{\omega}_a \sin(\omega_{ac}t) + \delta\boldsymbol{\omega}_b \cos(\omega_{ac}t), \quad (23)$$

which can be realized in practice by implementing two independent electric fields at the quantum dot site. This is, however, by no means necessary for our EDSR scheme.

The Rabi frequency then reads

$$\boldsymbol{\omega}_R = \frac{1}{2} (\delta\boldsymbol{\omega}_a \times \mathbf{n} - [\delta\boldsymbol{\omega}_b \times \mathbf{n}] \times \mathbf{n}). \quad (24)$$

Here, we assume that ω_{ac} is not far from resonance, *i.e.* $|\omega_{ac} - \omega_Z| < \omega_{ac}/2$. In a coordinate frame (X, Y, Z) with $Z \parallel \mathbf{B}$, the spin dynamics is approximated as follows

$$\langle S_{\pm}(t) \rangle \approx \tilde{S}_{\pm}(t) e^{\pm i\omega_{ac}t} \quad (25)$$

$$\langle S_Z(t) \rangle \approx \tilde{S}_Z(t), \quad (26)$$

where $S_{\pm} = S_X \pm iS_Y$. The spin $\tilde{\mathbf{S}}(t)$ obeys a simpler (static) Bloch equation

$$\dot{\tilde{\mathbf{S}}} = (\boldsymbol{\delta} + \boldsymbol{\omega}_R) \times \tilde{\mathbf{S}} - \tilde{\Gamma} \tilde{\mathbf{S}} + \tilde{\boldsymbol{\Upsilon}}, \quad (27)$$

where $\boldsymbol{\delta} = (\omega_Z - \omega_{ac})\mathbf{n}$ gives the detuning from resonance. The relaxation tensor $\tilde{\Gamma}_{ij}$ is diagonal, with $\tilde{\Gamma}_{XX} = \tilde{\Gamma}_{YY} = 1/T_2$ and $\tilde{\Gamma}_{ZZ} = 1/T_1$, and $\tilde{\Upsilon}_i$ assumes $\tilde{\Upsilon}_i = \tilde{\Gamma}_{ij} S_j^T$. Here, T_1 and T_2 are the relaxation and decoherence times in the absence of driving measured in experiment,^{24,25,31} and $\mathbf{S}^T = -(\mathbf{n}g/2|g|) \tanh(E_Z/2k_B T)$ is the thermodynamic value of spin, with T being the temperature.

The time-evolution of $\tilde{\mathbf{S}}$ in Eq. (27) is simplest in a coordinate frame (X', Y', Z') , with $Z' \parallel (\boldsymbol{\delta} + \boldsymbol{\omega}_R)$, and reads

$$\begin{aligned} \tilde{S}_{X'}(t) &= S_{\perp}^0 e^{-t/\tilde{T}_2} \sin\left(t\sqrt{\delta^2 + \omega_R^2} + \phi\right), \\ \tilde{S}_{Y'}(t) &= S_{\perp}^0 e^{-t/\tilde{T}_2} \cos\left(t\sqrt{\delta^2 + \omega_R^2} + \phi\right), \\ \tilde{S}_{Z'}(t) &= \tilde{S}_T + (S_{Z'}^0 - \tilde{S}_T) e^{-t/\tilde{T}_1}, \end{aligned} \quad (28)$$

where $S_{\perp}^0, S_{Z'}^0$, and ϕ give the initial spin state, $\langle \mathbf{S}(0) \rangle \equiv \tilde{\mathbf{S}}(0) = (S_{\perp}^0 \sin \phi, S_{\perp}^0 \cos \phi, S_{Z'}^0)$, in the coordinate frame (X', Y', Z') . Furthermore, the decay times \tilde{T}_1 and \tilde{T}_2 read

$$\begin{aligned} \frac{1}{\tilde{T}_1} &= \frac{1}{\delta^2 + \omega_R^2} \left(\frac{\delta^2}{T_1} + \frac{\omega_R^2}{T_2} \right), \\ \frac{1}{\tilde{T}_2} &= \frac{1}{2(\delta^2 + \omega_R^2)} \left(\frac{\omega_R^2}{T_1} + \frac{2\delta^2 + \omega_R^2}{T_2} \right). \end{aligned} \quad (29)$$

The stationary value of spin $\tilde{\mathbf{S}}_T := \tilde{\mathbf{S}}(t \rightarrow \infty)$ to leading order reads

$$\tilde{\mathbf{S}}_T = -\frac{g}{2|g|} \frac{(\boldsymbol{\delta} + \boldsymbol{\omega}_R)\delta}{\delta^2 + (T_1/T_2)\omega_R^2} \tanh(E_Z/2k_B T). \quad (30)$$

Note that at resonance ($\delta = 0$), the right-hand side in Eq. (30) vanishes. Therefore, in the vicinity of resonance, $\tilde{\mathbf{S}}_T$ is determined by the subleading order term, which can be obtained from Eq. (30) by replacing the numerator $(\boldsymbol{\delta} + \boldsymbol{\omega}_R)\delta \rightarrow (1/T_2)[\boldsymbol{\omega}_R \times \mathbf{n}]$. Measurement of $\tilde{\mathbf{S}}_T$ in the presence of driving provides information about the spin lifetimes $T_{1,2}$. For instance, at resonance the relaxation time T_1 can be accessed at the leading order of $\Gamma_{ij}/\omega_R \ll 1$,

$$\tilde{\mathbf{S}}_T(\delta = 0) = -\frac{g}{|g|} \frac{\boldsymbol{\omega}_R \times \mathbf{n}}{2T_1\omega_R^2} \tanh(E_Z/2k_B T). \quad (31)$$

Finally, we estimate the Rabi frequency ω_R using Eq. (24) and the parameters from Sec. III. For $\Omega_0 \sim 10^{-3}$, $|g| = 0.44$, and $B = 10 \text{ T}$ we obtain $\omega_R \sim 10^8 \text{ s}^{-1}$. We conclude that, with the present quantum-dot setups, EDSR enables one to manipulate the electron spin on a time scale of 10 ns, which is considerably shorter than the spin lifetimes, for which values between 1 and 150 ms (depending on the applied magnetic field) in gated GaAs quantum dots have been reported recently.^{24,31}

V. p^3 -DRESSELHAUS TERMS

Next we consider the so-called p^3 terms of the Dresselhaus spin-orbit interaction²³,

$$H_{SO} = \frac{\gamma}{2} (p_y p_x p_y \sigma_x - p_x p_y p_x \sigma_y), \quad (32)$$

where $\gamma = \alpha_c / \sqrt{2m_e^3 E_g}$ is the spin-orbit coupling constant, with α_c (≈ 0.07 for GaAs²³) being a dimensionless constant defined in Ref. 32 and E_g the band gap. For simplicity, we impose here the dipolar approximation for the ac -signal,

$$V(\mathbf{r}, t) = e \int_0^{\mathbf{r}} d\mathbf{r}' \cdot \mathbf{E}(\mathbf{r}', t) \approx e \mathbf{E}(t) \cdot \mathbf{r}. \quad (33)$$

Quite remarkably, if the quantum dot potential is harmonic, $U(\mathbf{r}) = \sum_{ij} u_{ij} r_i r_j$, then the spin does not couple to $\mathbf{E}(t)$ at the first order of H_{SO} and zeroth order of E_Z . Indeed, the second term in Eq. (11) vanishes for $V(\mathbf{r}, t) = e \mathbf{E}(t) \cdot \mathbf{r}$ and $S = \hat{L}_d^{-1} H_{SO}$ because of the following two identities

$$\langle \psi_0 | [\hat{L}_d^{-1} H_{SO}, \mathbf{r}] | \psi_0 \rangle = \langle \psi_0 | [\hat{L}_d^{-1} \mathbf{r}, H_{SO}] | \psi_0 \rangle, \quad (34)$$

$$[\hat{L}_d^{-1} \mathbf{r}, H_{SO}] = 0, \quad \forall H_{SO}(\mathbf{p}). \quad (35)$$

The latter is specific to H_d in Eq. (5) with a harmonic $U(\mathbf{r})$, for which the operator $\hat{L}_d^{-1} \mathbf{r}$ can be expressed via the components of $\mathbf{p} - (e/c) \mathbf{B}_z \times \mathbf{r}$. Note that, generally, $[\mathbf{p}, H_{SO}] = (e/c) [\mathbf{B}_z \times \mathbf{r}, H_{SO}]$ for any H_{SO} that is a function of only $\mathbf{p} = (p_x, p_y)$. Thus, for a harmonic confining potential, one is left with the same dominant mechanism as considered above for the "linear in p " terms. Expanding in terms of the Zeeman interaction, we recover Eqs. (13) and (14) with $\boldsymbol{\Omega}(t)$ given now by

$$\Omega_i(t) = -\frac{e}{m_e \omega_0^2} \sum_j (\lambda_{SO}^{-1})_{ij} E_j(t), \quad (36)$$

$$(\lambda_{SO}^{-1})_{ij} = \frac{m_e}{\hbar} \langle \psi_0 | \frac{\partial^2 H_{SO}}{\partial \sigma_i \partial p_j} | \psi_0 \rangle, \quad (37)$$

where $(\lambda_{SO}^{-1})_{ij}$ is a tensor of inverse spin-orbit lengths, and as before we consider $U(\mathbf{r}) = m_e \omega_0^2 r^2 / 2$. For H_{SO} in Eq. (32), we obtain explicitly $(\lambda_{SO}^{-1})_{ij} = \frac{1}{4} \gamma \omega_0 m_e^2 \delta_{ij}$ and $\Omega_i(t) = -\gamma e m_e E_i(t) / 4 \omega_0$. To estimate the strength of the resulting EDSR, we note that $\gamma \sim \beta d^2 / \hbar^2$, and therefore the amplitude of $\mathbf{h}(t) = 2g\mu_B \mathbf{B} \times \boldsymbol{\Omega}(t)$ is down now by a factor $d^2 / \lambda^2 \ll 1$ compared to the p -terms.

Next we consider a quantum dot with non-harmonic potential $U(\mathbf{r})$ and show that the p^3 -terms in Eq. (32) give rise to a spin-electric coupling proportional to the cyclotron frequency $\omega_c = eB_z / m_e c$. Since $\hbar \omega_c$ differs parametrically from E_Z ($E_Z / \hbar \omega_c = g m_e B / 2 m B_z$), the p^3 -terms can be as significant as the p -terms, provided $E_Z / \hbar \omega_c \lesssim d^2 / \lambda^2$, which is realistic for GaAs quantum dots. Note that for the p -terms no spin-electric coupling proportional to ω_c arises at the first order of H_{SO} . We

thus leave out \hat{L}_Z in Eq. (10) and consider a confining potential $U(\mathbf{r})$ that differs from a harmonic one by a function $W(\mathbf{r})$,

$$U(\mathbf{r}) = \sum_{ij} u_{ij} r_i r_j + W(\mathbf{r}) \equiv U_H(\mathbf{r}) + W(\mathbf{r}), \quad (38)$$

where u_{ij} are real coefficients and $W(\mathbf{r}) = \mathcal{O}(r^3)$. While in general $W(\mathbf{r})$ need not be small compared to $H_H = p^2 / 2m_e + U_H(\mathbf{r})$, in the following we expand the denominator of Eq. (10) in terms of $W \ll H_H$, considering therefore only small deviations of $U(\mathbf{r})$ from harmonic potentials. Then, using Eqs. (11), (13), and (33), we obtain at leading order in ω_c

$$\frac{h_i(t)}{\omega_c} = e \mathbf{E}(t) \cdot \langle \psi_0 | [\mathbf{R}(\mathbf{r}), \frac{\partial^2 S_H}{\partial \omega_c \partial \sigma_i}] | \psi_0 \rangle \Big|_{\omega_c=0}, \quad (39)$$

where we set $\omega_c \rightarrow 0$ in the right-hand side of Eq. (39) after evaluating $\partial S_H / \partial \omega_c$ in the symmetric gauge, with S_H defined as $[H_H, S_H] = H_{SO}$. The linear relationship between h_i and ω_c holds for $\omega_c \ll \omega_0$, where $\omega_0 \equiv 2\sqrt{\det(u)/m_e \text{Tr}(u)}$. In Eq. (39), the perturbation $W(\mathbf{r})$ enters via the function $\mathbf{R}(\mathbf{r})$ defined as follows

$$R_i(\mathbf{r}) = \sum_j (u^{-1})_{ij} \frac{\partial W(\mathbf{r})}{\partial r_j}. \quad (40)$$

Note that $\langle R/r \rangle \sim W_0 \lambda_d / \hbar \omega_0 \lambda_W$ is the small parameter of our expansion in terms of $W(\mathbf{r})$, with W_0 and $\lambda_W \lesssim \lambda_d$ being, respectively, the characteristic amplitude and length scale of the variation of $W(\mathbf{r})$ over the quantum dot size. It is important to note that the antisymmetric part of $W(\mathbf{r})$ drops out in Eq. (39) because H_{SO} is also antisymmetric with respect to $\mathbf{r} \rightarrow -\mathbf{r}$.

Next, as an example, we consider $U_H(\mathbf{r}) = m_e \omega_0^2 r^2 / 2$ and $W(\mathbf{r}) = \eta r^4$, and obtain

$$\frac{1}{2} \mathbf{h}(t) \cdot \boldsymbol{\sigma} = \frac{e \gamma \eta \hbar^2 \omega_c}{9 m_e \omega_0^4} (E_y(t) \sigma_x + E_x(t) \sigma_y). \quad (41)$$

Here, we have used the deformation quantization theory,³³ which allowed us to considerably simplify the derivation of Eq. (41) by performing most of the calculation in classical mechanics and only at the final stage come back to quantum mechanics. We have also carried out a fully quantum derivation of Eq. (41) and recovered the same result.

To estimate the strength of the resulting EDSR, we note that $\hbar \sim \hbar \omega_c (\lambda_d / \lambda_{SO}) (e \lambda_d E_0 / \hbar \omega_0) \langle R/r \rangle$, where $\lambda_{SO} = 4 / \gamma \omega_0 m_e^2$ ($\approx \lambda_d^2 / [0.01 \text{ nm}]$ for GaAs) is the spin-orbit length of the p^3 -terms and the parameter $\langle R/r \rangle \sim W(\lambda_d) / \hbar \omega_0$ characterizes the deviation of the quantum dot confinement from harmonic. In practice, $\langle R/r \rangle$ can be as large as unity, but here we assume $\langle R/r \rangle \sim \eta \lambda_d^4 / \hbar \omega_0 = 0.1$. For an electric field with amplitude $E_0 = 10^2 \text{ V/cm}$ and a GaAs quantum dot with $\hbar \omega_0 = 1 \text{ meV}$, we obtain the equivalent of an ac magnetic field $\delta \mathbf{B}(t) = \mathbf{h}(t) / g \mu_B$ that has an amplitude

$\delta B_0 \approx 1 \text{ mT}$ at $B_z = 1 \text{ T}$ and $|g| = 0.44$. In contrast to the previous mechanism, $\delta \mathbf{B}(t)$ can have here also a finite longitudinal component $\delta \mathbf{B}_{\parallel}(t) = \mathbf{n}(\mathbf{n} \cdot \delta \mathbf{B}(t))$, which however vanishes if $\mathbf{B} \parallel z$.

Finally, we note that the p^3 -terms can also be relevant for spin relaxation in quantum dots with non-harmonic confining potential. Of course, the magnetic field has to have an out-of-plane component for this spin-electric coupling to dominate over the one considered in Sec. III.

VI. DISCUSSIONS

The coupling of spin to electric fields that we have derived above can be used in a variety of ways to access and manipulate the electron spin in experiments. The effective Hamiltonian in Eq. (13) has the same form as the Hamiltonian of an ESR effect. This shows that ESR and EDSR are mutually interchangeable and the choice of the effect to be used depends on the particular experimental setup. In GaAs quantum dots, the spin-orbit interaction is weak enough to ensure long coherence times and, at the same time, strong enough to allow room for spin manipulation on an experimentally accessible timescale of $\sim 10 \text{ ns}$. Much shorter timescales can be achieved in InAs quantum dots, because of a much stronger spin-orbit coupling and a larger electron g -factor. In contrast, the EDSR effect is of little use in materials with very weak or nearly absent spin-orbit interaction, such as, e.g., carbon-nanotube quantum dots. To make order-of-magnitude estimates easier, we draw an analogy between the EDSR and ESR effects in terms of the particular way the \mathbf{B} and \mathbf{E} fields couple to the electron spin $\mathbf{S} = (\hbar/2)\boldsymbol{\sigma}$.

We recall that the ESR effect occurs as a result of the Zeeman interaction of the electron spin with an ac magnetic field. It is convenient to write this interaction in the form of a magnetic dipole interaction,

$$H_{\text{ESR}} = -\boldsymbol{\mu} \cdot \mathbf{B}(t), \quad (42)$$

where $\mathbf{B}(t)$ is the ac magnetic field and $\boldsymbol{\mu}$ is the electron magnetic moment,

$$\boldsymbol{\mu} = -\frac{1}{2}g\mu_B\boldsymbol{\sigma}, \quad (43)$$

where g is, in general, a tensor, see Eq. (A18).

By analogy with the ESR effect, the EDSR effect can be viewed as arising from an interaction between the ac electric field $\mathbf{E}(t)$ and a spin-electric moment $\boldsymbol{\nu}$. The respective spin-electric interaction is then analogous to Eq. (42) and reads

$$H_{\text{EDSR}} = -\boldsymbol{\nu} \cdot \mathbf{E}(t), \quad (44)$$

where the spin-electric moment $\boldsymbol{\nu}$ is due to an interplay between the spin-orbit interaction and some time-reversal breaking interaction, such as the Zeeman interaction. This analogy is not complete. Equation (44) is

valid only for ac electric fields $\mathbf{E}(t)$ that oscillate around zero, whereas Eq. (42) holds also for static B -fields. The reason why a static electric field \mathbf{E} cannot be used in Eq. (44) will become clear after we explain the origin of $\boldsymbol{\nu}$ in Eq. (44).

The spin-electric moment $\boldsymbol{\nu}$ arises because the dipolar transitions in the quantum dot become allowed, e.g., for the ground state

$$\langle \psi_{0\uparrow} | \mathbf{r} | \psi_{0\downarrow} \rangle \neq 0. \quad (45)$$

The electron charge density operator $\rho(\mathbf{r}) = -e\delta(\mathbf{r} - \mathbf{r}_{el})$, where \mathbf{r}_{el} is the electron coordinate, acquires spin-dependent terms in the transformed basis,

$$|\psi_{ns}\rangle = e^{-S}|\psi_n\rangle|\chi_s\rangle, \quad (46)$$

$$\tilde{\rho}(\mathbf{r}) = e^S \rho(\mathbf{r}) e^{-S}, \quad (47)$$

where e^{-S} is the transformation used in Section III and studied in detail in Appendix A. One can present $\tilde{\rho}(\mathbf{r})$ as a sum of two terms,

$$\tilde{\rho}(\mathbf{r}) = \bar{\rho}(\mathbf{r}) + \delta\rho(\mathbf{r}), \quad (48)$$

where $\bar{\rho}(\mathbf{r})$ is spin independent and $\delta\rho(\mathbf{r})$ is proportional to the spin. Then the spin-electric moment can be written as follows,

$$\boldsymbol{\nu} = \int \mathbf{r} \delta\rho(\mathbf{r}) dv, \quad (49)$$

where dv is the elementary volume of integration. Equation (49) unveils the physical meaning of the spin-electric moment $\boldsymbol{\nu}$: due to the mixed spin and orbit nature of the electron density, the electron spin couples to the first moment (dipole moment) of the electron.

While oscillating around an equilibrium position, the electron produces a time-dependent dipole moment, part of which is proportional to the electron spin. Obviously, in a static electric field, one can set to zero the electron dipole moment, because the new electron position can be taken as the equilibrium one. Therefore, only the change of the moment as a function of time has a physical meaning for single electrons (as for any other monopoles). In contrast, the electron magnetic moment $\boldsymbol{\mu}$ couples to static magnetic fields, because one can view $\boldsymbol{\mu}$ as arising from a pair of Dirac monopoles of opposite signs, for which the relative distance between them has an absolute meaning.

Equation (49) is written in a very general (operator) form. After taking the expectation value in the orbital ground state $|\psi_0\rangle$, we obtain

$$\boldsymbol{\nu} = -\frac{1}{2}\bar{\bar{\nu}}\boldsymbol{\sigma}, \quad (50)$$

$$\bar{\bar{\nu}}_{ij} = 2e \frac{\partial}{\partial \sigma_j} \langle \psi_0 | e^S r_i e^{-S} | \psi_0 \rangle, \quad (51)$$

where the derivative with respect to σ_j is defined as a usual derivative of an expression that is linear in $\boldsymbol{\sigma}$. Note

that Eq. (50) is analogous to Eq. (43) where the role of $g\mu_B$ is played by the tensor $\bar{\nu}$. Using Eqs. (13)-(15) we obtain for the linear in momentum spin-orbit interaction,

$$\bar{\nu}_{ij} = -\frac{2eg\mu_B}{m_e\omega_0^2}\varepsilon_{jkl}B_k(\lambda_{SO}^{-1})_{li}. \quad (52)$$

Similarly, for the p^3 Dresselhaus terms we obtain from Eq. (41)

$$\bar{\nu}_{ij} = \frac{2e\gamma\eta\hbar^2\omega_c}{9m_e\omega_0^4}\begin{pmatrix} 0 & 1 \\ 1 & 0 \end{pmatrix}, \quad (53)$$

where we use the coordinate frame (x, y) to represent the tensor. Note that in both cases $\bar{\nu}_{ij}$ is proportional to the magnetic field (or one of its components). The spin-orbit interaction produces no spin-electric coupling at $B = 0$, because of the time-reversal symmetry of spin-orbit interaction.

The analogy between μ and ν is also seen in the pairwise interaction between spins in separate (not tunnel coupled) quantum dots.³⁴ For an unscreened Coulomb interaction between electrons, the spin-spin interaction is analogous to the magnetic dipole-dipole interaction,³⁴

$$H_{dd} = \sum_{i < j} \frac{\nu_i \cdot \nu_j r_{ij}^2 - 3(\nu_i \cdot \mathbf{r}_{ij})(\nu_j \cdot \mathbf{r}_{ij})}{\kappa r_{ij}^5}, \quad (54)$$

where $\mathbf{r}_{ij} = \mathbf{r}_i - \mathbf{r}_j$ is the distance between two quantum dots ($r_{ij} \gg \lambda_d$) and κ is the electric permittivity of the material. For further detail and a microscopic derivation of Eq. (54) we refer the reader to Ref. 34.

Next we discuss the limitations of our theory. Throughout the paper, we have assumed that the spin orbit interaction is weak compared to the dot level spacing, or, in other words, that $\lambda_d/\lambda_{SO} \ll 1$. This assumption allowed us to use the perturbation theory to find the unitary transformation $\exp(-S)$, see Appendix A. Of course, this restriction was not necessary, if, e.g., we were to apply numerical methods to diagonalize the Hamiltonian. In particular, note that Eq. (49) is meaningful whenever the unitary transformation $\exp(-S)$ exists. The latter is always the case, including also extended states. Our perturbative results are qualitatively correct for $\lambda_d \lesssim \lambda_{SO}$ and can be used in experiments to estimate the strength of the EDSR effect. The case $\lambda_d \gg \lambda_{SO}$ is more seldom and requires a separate theoretical investigation.

As a second limitation, we would like to mention the adiabaticity criterion. In Sections III and V, we have derived effective Hamiltonians for the low energy subspace of the quantum dot Hilbert space. For the validity of this effective description, it is important that the switching (on and off) of the effective interaction occurs on a time scale that is larger than the inverse level spacing in the quantum dot. Obviously, this criterion excludes applicability of our theory to extended states. In practice, however, the finite temperature T imposes a more stringent criterion on the confinement energy, $\hbar^2/m_e\lambda_d^2 \gg k_B T$.

The third limitation of our theory is a small amplitude of oscillation of the quantum dot, $r_0/\lambda_{SO} \ll 1$. We have shown in Section III that the EDSR effect is proportional to this small parameter. Thus, for breaking the time-reversal symmetry by the Zeeman interaction we have (by order of magnitude)

$$\omega_R \sim \omega_Z \frac{r_0}{\lambda_{SO}}, \quad (55)$$

where $\omega_Z = E_Z/\hbar$. Similarly, for breaking the time-reversal symmetry by the orbital B -field effect (Section V), we have

$$\omega_R \sim \omega_c \frac{r_0}{\lambda_{SO}} \langle R/r \rangle, \quad (56)$$

where $\langle R/r \rangle$ is the small parameter of deviation of the quantum dot confinement from harmonic. We remark that our theory remains qualitatively valid also for $r_0/\lambda_{SO} \sim 1$ and for $\langle R/r \rangle \sim 1$. Beyond these limits, we do not expect the Rabi frequency to grow indefinitely. The Rabi frequency is bound in the case of Eq. (55) by $\omega_R \leq \omega_Z$, and in the case of Eq. (56) by $\omega_R \leq \omega_c$. We conclude that, by designing quantum dot setups that allow for large oscillation amplitudes $r_0 \lesssim \lambda_{SO}$, the EDSR effect can be strongly enhanced, beyond the numeric estimates made in Sections III, IV, and V.

In conclusion, the EDSR mechanisms presented above provides a means of implementing local electrical control of electron spins in quantum dots.

Acknowledgment

We thank M. Trif, L.M.K. Vandersypen, and D.M. Zumbühl for discussions. We acknowledge support from the Swiss NSF, NCCR Nanoscience, DARPA, ONR, and JST ICORP.

APPENDIX A: SCHRIEFER-WOLFF TRANSFORMATION AND FINE STRUCTURE

In this Appendix, we first work out the Schrieffer-Wolff transformation to the third order of perturbation theory and for a general weak perturbation. Then, we consider an example Hamiltonian and use the Schrieffer-Wolff transformation to partly diagonalize the Hamiltonian. Finally, we analyze the fine structure of the transformed Hamiltonian and complete its diagonalization by an additional unitary transformation.

As in standard perturbation theory, we consider a Hamiltonian $H = H_0 + H_1$, where H_1 is a weak perturbation with respect to H_0 . For the matrix elements of H_1 , we assume

$$\langle n|H_1|m \rangle = 0, \quad \text{for } E_n = E_m, \quad (A1)$$

$$\langle n|H_1|m \rangle \ll E_n - E_m, \quad \text{for } E_n \neq E_m, \quad (A2)$$

where $|n\rangle$ and E_n are, respectively, the eigenstates and eigenvalues of H_0 , and are obtained from $H_0|n\rangle = E_n|n\rangle$.

The projector \mathcal{P} , defined as follows

$$\mathcal{P}A = \sum_{\substack{n,m \\ E_n=E_m}} A_{nm}|n\rangle\langle m|, \quad \forall A \quad (\text{A3})$$

projects onto the diagonal or degenerate part of H_0 . In the particular case, when the spectrum of H_0 is non-degenerate, \mathcal{P} assumes $\mathcal{P}A = \sum_n A_{nn}|n\rangle\langle n|$, $\forall A$. From Eq. (A1) and the definition (A3), it follows that

$$\mathcal{P}H_1 = 0, \quad (\text{A4})$$

$$\mathcal{P}H_0 = H_0. \quad (\text{A5})$$

Next we look for a unitary transformation that brings the Hamiltonian $H = H_0 + H_1$ to a partly diagonal form,

$$\tilde{H} = e^{S'}(H_0 + H_1)e^{-S'} = H_0 + \Delta H, \quad (\text{A6})$$

where the operator ΔH obeys $\mathcal{P}\Delta H = \Delta H$. Here, $S' = -S'^\dagger$ is the transformation matrix. The unitary transformation in Eq. (A6) is called the Schrieffer-Wolff transformation.³⁵ We expand S' and ΔH in terms of the perturbation H_1 :

$$S' = S'^{(1)} + S'^{(2)} + S'^{(3)} + \dots, \quad (\text{A7})$$

$$\Delta H = \Delta H^{(1)} + \Delta H^{(2)} + \Delta H^{(3)} + \dots, \quad (\text{A8})$$

where the superscripts give the order of perturbation theory. Substituting Eqs. (A7) and (A8) into Eq. (A6), we find a set of equations for S' ,

$$[H_0, S'^{(1)}] = H_1, \quad (\text{A9})$$

$$[H_0, S'^{(2)}] = \frac{\mathcal{Q}}{2}[S'^{(1)}, H_1], \quad (\text{A10})$$

$$[H_0, S'^{(3)}] = \frac{\mathcal{Q}}{2}[S'^{(2)}, H_1] + \frac{\mathcal{Q}}{12}[S'^{(1)}, [S'^{(1)}, H_1]] + \frac{\mathcal{Q}}{4}[S'^{(1)}, \mathcal{P}[S'^{(1)}, H_1]], \quad (\text{A11})$$

where $\mathcal{Q} \equiv 1 - \mathcal{P}$. It is important to note that S is defined in Eqs. (A9)-(A11) up to terms $\mathcal{P}M$, where M is arbitrary. Such terms drop out on the left-hand side in Eqs. (A9)-(A11) because $[H_0, \mathcal{P}S'] = 0$. Thus, $\mathcal{P}S'$ can be chosen arbitrarily, which shows that there are infinitely many transformation matrices S' that satisfy Eq. (A6). For simplicity, we choose $\mathcal{P}S' = 0$ and address the fine structure of $\tilde{H} = H_0 + \Delta H$ later on. For the operator ΔH , we obtain

$$\Delta H^{(1)} = 0, \quad (\text{A12})$$

$$\Delta H^{(2)} = \frac{\mathcal{P}}{2}[S'^{(1)}, H_1], \quad (\text{A13})$$

$$\Delta H^{(3)} = \frac{\mathcal{P}}{3}[S'^{(1)}, [S'^{(1)}, H_1]]. \quad (\text{A14})$$

Introducing the Liouvillean \hat{L}_0 : $\hat{L}_0 A = [H_0, A]$, $\forall A$, we can formally solve Eqs. (A9)-(A11) one by one. For

example, the transformation matrix at the lowest order reads $S'^{(1)} = \mathcal{Q}\hat{L}_0^{-1}H_1$. For ΔH , we recover then the perturbation theory expansion in a more familiar form,

$$\Delta H = -\mathcal{P}H_1\hat{L}_0^{-1}H_1 + \mathcal{P}H_1\hat{L}_0^{-1}H_1\hat{L}_0^{-1}H_1 + \dots, \quad (\text{A15})$$

with the usual convention, $\mathcal{P}\hat{L}_0^{-1}A = 0$, $\forall A$, adopted.

Next, we remark that the fine structure of $\tilde{H} = H_0 + \Delta H$ can be addressed in each particular case by means of degenerate perturbation theory. As an example, we consider here the Hamiltonian $H = H_0 + H_1$, with $H_0 = H_d + H_Z$ and $H_1 = H_{SO}$. Here, H_d is given in Eq. (5), with $U(\mathbf{r}) = m_e\omega_0^2 r^2/2$, H_Z is given in Eq. (6), and H_{SO} is given in Eq. (7). Using the transformation matrix $S' = S$, with S given in Eq. (12), we obtain a diagonal Hamiltonian, $\tilde{H} = H_d + H_Z$, at the first order of H_{SO} . At the second order of H_{SO} , however, a fine structure in the energy spectrum arises. At $B = 0$, the transformed Hamiltonian reads

$$\tilde{H} = \frac{p^2}{2m_e} + \frac{m_e\omega_0^2}{2}r^2 + \frac{1}{2}\Delta_{SO}\ell_z\sigma_z, \quad (\text{A16})$$

where $\ell_z = -i(x\partial/\partial y - y\partial/\partial x)$ is the electron rotational momentum and $\Delta_{SO} = 2m_e(\beta^2 - \alpha^2)$. The Kramers doublets are identified, in this case, as the pairs of states with quantum numbers (ℓ_z, σ_z) and $(-\ell_z, -\sigma_z)$. For $\ell_z > 0$, the two-fold orbital degeneracy is lifted and a splitting $\Delta_{SO}\ell_z$ arises. Note that the ground orbital state, which has $\ell_z = 0$, remains doubly degenerate in this case.

At $B \neq 0$, the fine-structure interaction in Eq. (A16) is modified by both the Zeeman energy E_Z and the cyclotron frequency ω_c . For simplicity, we omit terms $\sim \Delta_{SO}E_Z/\hbar\omega_0$, but keep terms $\sim \Delta_{SO}\omega_c/\omega_0$, assuming that $E_Z \ll \hbar\omega_c$. Then, the Hamiltonian (A16) acquires two extra terms

$$\frac{E_Z}{2}\mathbf{n} \cdot \boldsymbol{\sigma} + \frac{\Delta_{SO}}{4\lambda^2}\sigma_z\mathcal{P}r^2, \quad (\text{A17})$$

where $\lambda = \sqrt{\hbar/m_e\omega_c}$ is the magnetic length and we use the symmetric gauge, $\mathbf{A}(\mathbf{r}) = B_z(-y/2, x/2, 0)$. The last term in Eq. (A17) can be viewed as a renormalization of the electron g -factor. Allowing for an anisotropic Zeeman interaction,

$$H_Z^{\text{eff}} = \frac{1}{2}\mu_B \sum_{ij} g_{ij}\sigma_i B_j, \quad (\text{A18})$$

we obtain that the tensor g_{ij} is diagonal in the main crystallographic frame, with

$$g_{xx} = g_{yy} = g, \quad g_{zz} = g + \frac{m\Delta_{SO}}{\hbar^2}\langle\psi_n|r^2|\psi_n\rangle, \quad (\text{A19})$$

where m is the electron mass in vacuum and ψ_n is the electron orbital state. For the ground orbital state, the corrected g -factor reads $g_{zz} = g + m\Delta_{SO}/m_e\hbar\omega$, where $\omega = \sqrt{\omega_0^2 + \omega_c^2}/4$. Note that the sign of the correction is

given by the sign of $\beta^2 - \alpha^2$ contained in Δ_{SO} . The spin quantization axis does not, in general, coincide with the magnetic field direction \mathbf{n} and is given by the following unit vector

$$\tilde{\mathbf{n}} = \frac{\mathbf{n} + \zeta \mathbf{n}_z}{\sqrt{1 + \zeta(2 + \zeta)n_z^2}}, \quad (\text{A20})$$

where $\zeta = (g_{zz} - g)/g$. An additional unitary transformation can be used to diagonalize the 2×2 blocks of Zeeman-split Kramers doublets,

$$\tilde{H}_Z^{\text{eff}} = e^{S''} H_Z^{\text{eff}} e^{-S''} = \frac{1}{2} \tilde{E}_Z \mathbf{n} \cdot \boldsymbol{\sigma} \quad (\text{A21})$$

where $\tilde{E}_Z = E_Z \sqrt{1 + \zeta(2 + \zeta)n_z^2}$ is the renormalized Zeeman energy and

$$e^{-S''} = \sqrt{\frac{1 + \mathbf{n} \cdot \tilde{\mathbf{n}}}{2}} - i \frac{\zeta[\mathbf{n} \times \mathbf{n}_z] \cdot \boldsymbol{\sigma}}{\sqrt{\zeta^2 n_z^2 (1 - n_z^2)}} \sqrt{\frac{1 - \mathbf{n} \cdot \tilde{\mathbf{n}}}{2}}. \quad (\text{A22})$$

So far, we have considered a given orbital state ψ_n , for which the tensor g_{ij} is given in Eq. (A19). The transformation above is also valid in general, provided ζ is understood as a diagonal operator, $\zeta = (m\Delta_{SO}/\hbar^2)\mathcal{P}r^2$.

We summarize by mentioning that the unitary transformation in Eq. (A6) can, in principle, be adjusted to give a fully diagonal $\tilde{H} = H_0 + \Delta H$, i.e. we had not to require $\mathcal{P}S' = 0$ in the first place. However, in practice, it is more convenient first to apply the non-degenerate perturbation theory, Eqs. (A9)-(A15), and then, at the end, complete the diagonalization of $H_0 + \Delta H$ by a second unitary transformation. The latter is specific to each particular case and amounts, in general, to applying the degenerate perturbation theory. For the sake of simplicity, we shall refer to S in the main text of the paper as to the full transformation matrix, despite the fact that the respective unitary transformation comes, in practice, as a product of two unitary transformations. Thus, we denote the product $e^{-S'} e^{-S''}$ by e^{-S} in the main text. Finally, we remark that $e^{-S''} \approx 1 + \mathcal{O}(H_{SO}^2)$.

-
- ¹ S.A. Wolf, D.D. Awschalom, R.A. Buhrman, J.M. Daughton, S. von Molnár, M.L. Roukes, A.Y. Chtchelkanova, and D.M. Treger, *Science* **294**, 1488 (2001).
 - ² *Semiconductor Spintronics and Quantum Computation*, D.D. Awschalom, D. Loss, and N. Samarth (eds.), (Springer, Berlin, 2002).
 - ³ D. Loss and D.P. DiVincenzo, *Phys. Rev. A* **57**, 120 (1998).
 - ⁴ N.M. Atherton, *Electron Spin Resonance*, (Ellis Horwood Limited, New York, 1973).
 - ⁵ H.-A. Engel and D. Loss, *Phys. Rev. Lett.* **86**, 4648 (2001); *Phys. Rev. B* **65**, 195321 (2002).
 - ⁶ Y. Kato, R.C. Myers, D.C. Driscoll, A.C. Gossard, J. Levy, and D.D. Awschalom, *Science* **299**, 1201 (2003).
 - ⁷ R.C. Miller, A.C. Gossard, D.A. Kleinman, and O. Munteanu *Phys. Rev. B* **29**, 3740 (1984).
 - ⁸ G. Salis, Y. Kato, K. Ensslin, D.C. Driscoll, A.C. Gossard, and D.D. Awschalom, *Nature (London)* **414**, 619 (2001).
 - ⁹ E.I. Rashba and A.L. Efros, *Phys. Rev. Lett.* **91**, 126405 (2003); *Appl. Phys. Lett.* **83**, 5295 (2003); E.I. Rashba, *J. Supercond. Incomp. Novel. Magn.* **18**, 137, (2005).
 - ¹⁰ G. Dresselhaus, *Phys. Rev.* **100**, 580 (1955).
 - ¹¹ Y. Bychkov and E. I. Rashba, *J. Phys. C* **17**, 6039 (1984).
 - ¹² R.L. Bell, *Phys. Rev. Lett.* **9**, 52 (1962).
 - ¹³ B.D. McCombe, S.G. Bishop, and R. Kaplan, *Phys. Rev. Lett.* **18**, 748 (1967).
 - ¹⁴ M. Dobrowolska, H.D. Drew, J.K. Furdyna, T. Ichiguchi, A. Witowski, and P.A. Wolff, *Phys. Rev. Lett.* **49**, 845 (1982); M. Dobrowolska, A. Witowski, J.K. Furdyna, T. Ichiguchi, H.D. Drew, and P.A. Wolff, *Phys. Rev. B* **29**, 6652 (1984).
 - ¹⁵ M. Schulte, J.G.S. Lok, G. Denninger, and W. Dietsche, *Phys. Rev. Lett.* **94**, 137601 (2005).
 - ¹⁶ M. Duckheim and D. Loss, *Nature Physics* **2**, 195 (2006).
 - ¹⁷ Y. Kato, R.C. Myers, A.C. Gossard, and D.D. Awschalom, *Nature (London)* **427**, 50 (2004).
 - ¹⁸ J. Nitta, T. Akazaki, H. Takayanagi, and T. Enoki *Phys. Rev. Lett.* **78**, 1335 (1997).
 - ¹⁹ L.P. Kouwenhoven, D.G. Austing, and S. Tarucha, *Rep. Prog. Phys.* **64** 701 (2001).
 - ²⁰ A.V. Khaetskii and Yu.V. Nazarov, *Phys. Rev. B* **61**, 12639 (2000); B.I. Halperin, A. Stern, Y. Oreg, J.N.H.J. Cremers, J.A. Folk, and C.M. Marcus, *Phys. Rev. Lett.* **86**, 2106 (2001); I.L. Aleiner and V.I. Fal'ko, *Phys. Rev. Lett.* **87**, 256801 (2001).
 - ²¹ V.N. Golovach, A. Khaetskii, and D. Loss, *Phys. Rev. Lett.* **93**, 016601 (2004).
 - ²² A.V. Khaetskii and Yu.V. Nazarov, *Phys. Rev. B* **64**, 125316 (2001).
 - ²³ M.I. D'yakonov and V.Yu. Kachorovskii, *Sov. Phys. Semicond.* **20**, 110 (1986).
 - ²⁴ J.M. Elzerman, R. Hanson, L.H. Willems van Beveren, B. Witkamp, L.M.K. Vandersypen, and L.P. Kouwenhoven, *Nature (London)* **430**, 431 (2004).
 - ²⁵ M. Kroutvar, Y. Ducommun, D. Heiss, M. Bichler, D. Schuh, G. Abstreiter, and J.J. Finley, *Nature (London)* **432**, 81 (2004).
 - ²⁶ J.D. Jackson, *Classical Electrodynamics*, (John Wiley & Sons, Inc., New York, 1999).
 - ²⁷ F.H.L. Koppens, C. Buizert, K.J. Tielrooij, I.T. Vink, K.C. Nowack, T. Meunier, L.P. Kouwenhoven, and L.M.K. Vandersypen, *Nature (London)* **442**, 766 (2006).
 - ²⁸ M. Borhani, V.N. Golovach, and D. Loss, *Phys. Rev. B* **73**, 155311 (2006).
 - ²⁹ F. Bloch, *Phys. Rev.* **70**, 460 (1946); R. K. Wangsness and F. Bloch, *Phys. Rev.* **89**, 728 (1953); F. Bloch, *Phys. Rev.* **105**, 1206 (1957).
 - ³⁰ C. Cohen-Tannoudji, B. Diu, and F. Laloë, *Quantum Mechanics*, Vol. II (John Wiley & Sons, New York, 1977).
 - ³¹ S. Amasha, K. MacLean, I. Radu, D.M. Zumbuhl, M.A. Kastner, M.P. Hanson, and A.C. Gossard, cond-mat/0607110.
 - ³² G.E. Pikus and A.N. Titkov, in *Optical orientation*, edited by F. Meier and B.P. Zakharchenya (North-Holland, Amsterdam, 1984).

- ³³ F. Bayen, M. Flato, C. Fronsdal, A. Lichnerowicz, and D. Sternheimer, *Ann. Phys.* **111**, 61 (1978); *Ann. Phys.* **111**, 111 (1978).
- ³⁴ M. Trif, V.N. Golovach, and D. Loss, cond-mat/0608512.
- ³⁵ J.R. Schrieffer, P.A. Wolff, *Phys. Rev.* **149**, 491 (1966).